



HAL
open science

Energy Consumption of Control Schemes for the Pioneer 3DX Mobile Robot: Models and Evaluation

Lotfi Jaïem, Didier Crestani, Lionel Lapierre, Sébastien Druon

► To cite this version:

Lotfi Jaïem, Didier Crestani, Lionel Lapierre, Sébastien Druon. Energy Consumption of Control Schemes for the Pioneer 3DX Mobile Robot: Models and Evaluation. *Journal of Intelligent and Robotic Systems*, 2021, 102 (1), pp.23. 10.1007/s10846-021-01374-6 . lirmm-04073356

HAL Id: lirmm-04073356

<https://hal-lirmm.ccsd.cnrs.fr/lirmm-04073356>

Submitted on 27 Apr 2023

HAL is a multi-disciplinary open access archive for the deposit and dissemination of scientific research documents, whether they are published or not. The documents may come from teaching and research institutions in France or abroad, or from public or private research centers.

L'archive ouverte pluridisciplinaire **HAL**, est destinée au dépôt et à la diffusion de documents scientifiques de niveau recherche, publiés ou non, émanant des établissements d'enseignement et de recherche français ou étrangers, des laboratoires publics ou privés.



Energy Consumption of Control Schemes for the Pioneer 3DX Mobile Robot: Models and Evaluation

Lotfi Jaiem¹ · Didier Crestani¹ · Lionel Lapierre¹ · Sébastien Druon¹

Received: 8 January 2020 / Accepted: 23 March 2021
 © Springer Nature B.V. 2021

Abstract

Energy is a key feature that must be explicitly managed for long-term autonomous robotic missions. Many research studies have addressed the energy issue, developed energy-aware motion control or integrated energy in mission objectives. However, few studies have comprehensively assessed the impact of software and hardware choices on power consumption of robots. Based on experimental analysis and according to the selected control scheme and hardware configuration, this paper proposes energy consumption models for the Pioneer 3DX. The proposed models highlight the existence of an optimal velocity that minimizes motion energy. These models are experimentally evaluated and discussed.

Keywords Robot energy consumption · Laptop energy consumption · Energy model evaluation · P3DX robot

1 Introduction

Mobile robotics aims at addressing a large range of mission classes. Unlike industrial robotics, the available embedded energy is limited for autonomous robots. Each robot decision has a direct impact on its energy stock and consequently on its operational capability to perform long-term missions. Energy is hence a key issue with regard to autonomous mobile robotic missions. Many research studies have focused on minimizing energy consumption. However few studies have dealt with the prediction of the energy consumption for various mission tasks according to the software and hardware resources involved. The availability of such models is essential to be able to efficiently manage real autonomous robotic missions. The definition of such models is the main topic of this paper.

Energy is a pivotal issue in autonomous robotics [3]. Research on this topic can be roughly divided into three main complementary levels: component, robot system and mission levels.

The *component level* aims to reduce energy consumption using energy-aware hardware or software techniques using Dynamic Power Management (DPM) techniques [4]. At the *robot system level* the goal is to model the robot's energy consumption according to a considered robotic task and trajectory. Finally, the *mission level* intends to model the mission energy consumption, using robot system energy information, according to the mission plan.

The energy issue has been less addressed at the robot system level. It is a difficult issue and most of autonomous robotic studies usually neglect the energy problem. Some studies focus on energetic optimality of locomotion strategy (e.g. legged robots [30], or snake like systems [13]). Here we are not addressing this question since our goal is to tackle the global energetic consumption at the mission level. In that context, short-term mission generally considers that the system embeds sufficient amount of energy to realize the planned tasks. However, it becomes a key issue when long-term or hazardous missions are concerned.

The robot system level is needed crossing point to address the mission level. Previous studies mainly focused on the identification of robot energy consumption model along energy-aware trajectories, for missions involving only a unique control task. Mei in [19] conducted an experimental analysis of power consumption of a Pioneer 3DX mobile robot, considering the motion energy, the sensors, and the computer consumption. Several studies have focused on the determination of optimal velocity profiles minimizing energy consumption, along predefined

✉ Lionel Lapierre
 lapierre@lirmm.fr

¹ Laboratoire d'Informatique Robotique et Microélectronique de Montpellier (LIRMM), UMR 5506, Université de Montpellier, C.N.R.S., 161 rue Ada, 34 095 Montpellier Cedex 5, Montpellier, France

48 trajectories. Kim and Kim in [14] focused on straight-line
 49 motion on flat surfaces. The same issue was addressed
 50 in Tokekar et al. [27, 28]. Different problems have been
 51 considered from a single segment to a path composed
 52 of N segments of straight lines and curves. Mei et al.
 53 in [31] explored different motion plan scenarios (scan
 54 lines, spiral square spirals) to cover an open area from
 55 an energy viewpoint to determine the most efficient one.
 56 Energy prediction approaches integrating rolling resistance
 57 for unmanned ground vehicles was addressed by Sadrpour
 58 et al. in [23] [24] and [25] using mission prior knowledge
 59 (road grade and rolling resistance information, driving style,
 60 etc.). These approaches were used in [9] to build an energy
 61 efficient coverage plan for ground robot, where simulation
 62 results were presented. Finally, in [21], an on-line prediction
 63 model for energy consumption of a Khepera III robot
 64 integrating the impact of the sensors was presented and
 65 experimentally evaluated on a very short mission.

66 Several experimental analyses of energy consumption
 67 have been published but this work aims to propose a generic
 68 formulation of the energy power consumption at the robot
 69 system level considering the different control schemes (CS)
 70 and their associated hardware and software resources. The
 71 main contributions are the following:

- 72 • We are considering a predictive energy consumption
- 73 model at the robot system level.
- 74 • We are considering here a multiple batteries system,
- 75 one devoted to the platform, the other supplying the
- 76 on-board laptop.
- 77 • This study enlightens in detail the software impact of the
- 78 algorithms selection on the energy consumption.
- 79 • A new model involving motion energy consumption,
- 80 velocity and covered distance, for a straight line path is
- 81 proposed for a Pioneer P3DX.
- 82 • Finally, most studies concerning energy consumption
- 83 models evaluate them locally on rather short robot
- 84 motion pathways. It is however essential to estimate
- 85 their accuracy along longer and more complex mis-
- 86 sions. This accuracy must remain acceptable to be

able to efficiently manage energy consumption at the 87
 mission level. 88

The paper is organized as follows. Section 2 presents 89
 first the hardware and software architectures and the 90
 experimental environment used. A general flowchart of the 91
 proposed method is provided and a generic formulation of 92
 the power consumption is exposed. In a first step, Section 3 93
 builds the models proposed for the architecture components 94
 as part of the previous generic formulation, and compares 95
 them to previous studies. In a second step, the accuracy of 96
 the generic model is evaluated according to a simple forward 97
 motion or a more complex patrolling mission. Finally the 98
 last section draws general and specific conclusions about 99
 this study. It also shows that the proposed study can address 100
 the energy management at the mission level and exposes 101
 some on going works. 102

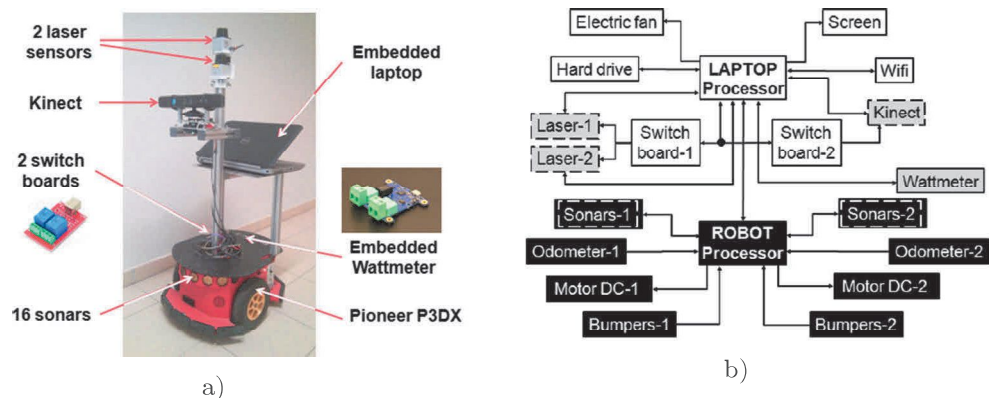
**2 Experimental Context and Proposed 103
 Methodology 104**

**2.1 The Robotic Platform and the Control 105
 Architecture 106**

Based on a classic Pioneer 3DX mobile robot, the robot 107
 platform (Fig. 1a) of 25 kg weight was equipped with many 108
 additional sensors and electronic devices to be able to imple- 109
 ment different motion, location and image analysis control 110
 schemes, and to perform online energy monitoring. 111

The two top to tail URG-04 LX Hokuyo 240°lasers 112
 (LAS) allow 360° scanning of the surrounding environment. 113
 A camera (Kinect®) system (KIN) is used to perform image 114
 analysis. Two added switchboards with two command 115
 channels allow for independent connection or disconnection 116
 of the power supply of the two laser devices and the camera, 117
 according to the chosen control scheme. An embedded 118
 USB wattmeter (Yocto-Watt) was also integrated to perform 119
 online measurements of the energy delivered by the robot 120
 battery. 121

Fig. 1 The Pioneer P3DX. **a**
 The robotic platform. **b** The
 hardware architecture



122 The on-board laptop supports a Linux-RTAI operating
 123 system, running the control architecture according to the
 124 Real-Time middleware ConTract [22] managing the control
 125 scheme selection during autonomous robotic missions. Its bat-
 126 tery supplies the laptop processor, screen, wifi board, hard
 127 drive and electric fan. It also supports USB communica-
 128 tion with the lasers, Kinect, switchboards, wattmeter and the
 129 robot micro-controller. The laptop battery consumption is
 130 estimated using the Linux *uevent* system file of the battery
 131 state. This file allows for on-line monitoring of the bat-
 132 tery current and voltage, and an estimation of the remaining
 133 laptop battery energy.

134 The hardware architecture of the robotic platform is
 135 presented in Fig. 1b. Elements supplied by the robot battery
 136 indicated with black boxes, while those supplied by the
 137 laptop battery are white boxes. Switchable components
 138 (switching on/off the electric supply) are shown with dotted
 139 lines. Furthermore, note that these components and the
 140 wattmeter are connected to the laptop using USB for data
 141 exchange, but are supplied by the robot battery (grey boxes).

142 A robotic mission can be divided into a set of potential
 143 overlapped areas where different robotic tasks (moving for-
 144 ward, communicating, locating, etc.) take place. A robotic
 145 task requires periodic call up of sensor information, con-
 146 trol or processing algorithms gathered in a control scheme.
 147 The control architecture managed the following control
 148 schemes, which involves specific sensors and algorithms.:

- 149 • Simple path following (SPF) with obstacle avoidance
 150 (using 1, 2 lasers or sonars), as described in [18].
- 151 • Centring motion (CM), where the system uses proximity
 152 measurements to follow the central line of a corridor.
- 153 • Dead-reckoning navigation using odometers (ODO).

- 154 • Navigation using grid-based localization (GBL) using 2
 155 top to tail lasers.
- 156 • QR-code navigation (QRCN), allowing the system to
 157 regularly control the estimation of its position using a
 158 camera.
- 159 • Image analysis (IA) performs a visual analysis of an
 160 image of a valve to obtain its status (open/close).

161 The hardware and software context of the study being
 162 presented, a generic formulation of the power consumption
 163 of a control scheme is now proposed (Table 1). Q5

164 **2.2 Power and Energy Consumption Models: Generic**
 165 **Formulation**

166 In the following we adapt the formulation proposed in [21]
 167 for a Khepera robot. Generally the instantaneous power con-
 168 sumption $P(CS)$ for a given CS can be divided into dynamic
 169 and static parts. The dynamic part P_{Dyn} denotes the *time-*
 170 *varying* power consumption. For example, motion power
 171 consumption depends on the chosen velocity and sonar
 172 power consumption depends on the chosen frequency rate.
 173 The static part P_{Stat} denotes the constant steady state power
 174 consumption of components like some sensors or communi-
 175 cation devices. Depending on the components recruited for
 176 a CS , the corresponding instantaneous consumption may
 177 significantly change, as Eq. 1 denotes.

$$P(CS) = \sum_{i=1}^{n_1} \alpha_i \cdot P_{Dyn\ i} + \sum_{j=1}^{n_2} \beta_j \cdot P_{Stat\ j} \quad (1)$$

178 Where n_1 is the number of dynamic components, n_2 the
 179 number of static components, while α_i and β_j are 1 if the

Table 1 Control schemes and hardware components (o: optional, •: required)

Control schemes	Software	Hardware					
		Control & Guidance	Navigation	Sensors			Actuators
				Sonars	Lasers	Camera	
FM	Forward Motion			o	o	o	•
SPF-OA	Path-following with obstacle avoidance		ODO	o	o-o	-	•
			QRCN	o	o-o	•	
			GBL	o	•-•		
CM-OA	Reactive centring control with obstacle avoidance		ODO	o	•-•	-	•
			QRCN	o	•-•	•	
RVT	Rotational visual tracking					•	•
IA	Image Analysis	-	-	-	-	•	-

The o-o symbol means that one of the two laser devices can be optionally chosen and the •-• symbol means that the two laser devices are required

180 considered component is involved in the current CS and 0
181 otherwise.

182 The energy consumption of a CS (Eq. 2) conventionally
183 obtained by multiplying the instantaneous power consump-
184 tion by the active duration ΔT of a CS .

$$E(CS) = P(CS) \cdot \Delta T(CS) \quad (2)$$

185 Based on this formulation, for the robot battery,
186 according to the hardware architecture and the selected
187 control scheme $CS \in \{FM, SPF, CM, RVT, IA\}$ the
188 following equation can be proposed:

$$P(CS) = \alpha_1 P_{R_{Motion}}(v) + \alpha_2 \cdot P_{R_{US}}(f) + \beta_1 \cdot P_{R_{Kinect}} + k_1 \cdot \beta_2 \cdot P_{R_{Laser}} \quad (3)$$

189 Where $k_1 \in \{0, 1, 2\}$ denotes the number of active lasers.
190 α_i (dynamic) and β_i (static) are Boolean coefficients that
191 indicate if the corresponding component is used or not.

192 For the laptop battery Eq. 1 can be developed in Eq. 4, for
193 the considered platform, according to the selected control
194 scheme CS and the external device connections EC (sensors,
195 switchboards, Kinect).

$$P_L(CS) = P_{L_{Proc}}(CS, EC) + P_{L_{Robot}} + P_{L_{Watt}} + \beta_1 \cdot P_{L_{Screen}} + \beta_2 \cdot P_{L_{Kinect}} + k_1 \cdot \beta_3 \cdot P_{L_{Laser}} + \beta_4 \cdot P_{L_{Switch_1}}(k_2) + \beta_5 \cdot P_{L_{Switch_2}}(k_3) \quad (4)$$

196 Where:

197 β_1 to β_5 are Boolean coefficients representing the
198 connection, or not, with corresponding external devices.

199 $k_1 \in \{1, 2\}$ represents the number of connected lasers.

200 $k_2 \in \{0, 1, 2\}$ represents the number of external devices
201 connected with the processor via the switchboard 1. 0, 1 or
202 2 lasers can be connected.

203 $k_3 \in \{0, 1, 2\}$ denotes the number of external devices
204 connected to the processor via the switchboard 2. 0 for
205 no connection and 1 for the Kinect connection. 2 is still
206 available for another connection.

207 So, the problem now is to identify independently each
208 part of these models.

2.3 Instantaneous Power Consumption: The Proposed Process

211 To determine the instantaneous power consumption the
212 followed process summarized in Fig. 2, can be decomposed
213 into the following steps.

- 214 1. The process can be done for each separate supplying
215 battery.
- 216 2. A detailed analysis of the hardware architecture allows
217 to put in light the hardware components physically
218 linked with a battery according to the different Control
219 Schemes. Static components can be distinguished from
220 the dynamic ones.

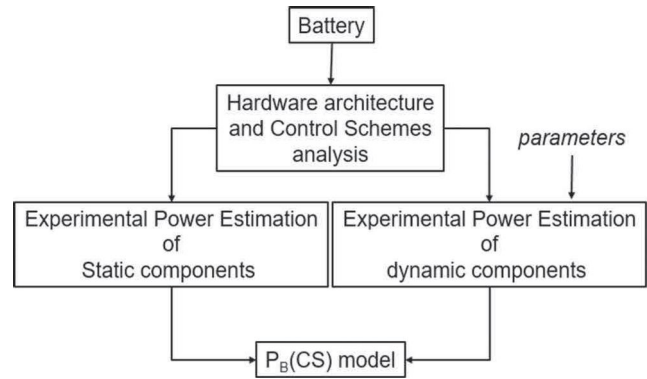


Fig. 2 Experimental process for power consumption identification

3. Depending on the component class, two different approaches must be used:

- The constant consumption of the static components can be measured externally using adapted wattmeter/current/voltage measurement devices. For a robot the component consumption can also be measured directly in situ using an embedded wattmeter. For a laptop, if the access to the battery is not easy, the power consumption can be measured on-line using dedicated software functions of monitoring.
- For the dynamic components the first work is to identify the relevant parameters influencing the power consumption using for example Ishikawa diagrams [10]. Sometimes a theoretical analysis can be engaged where acceptable simplifying assumptions must be adopted. Then these parameters must be tuned to determine the consumption behaviour using adapted experimental procedure.

4. Once the power consumption identification is completed, the generic formulation (Eqs. 3 and 4) of the battery power consumption P_B is obtained.

Finally, the last step is to estimate the accuracy of the proposed formulations.

2.4 Energy Models Evaluation: Experimental Context

To validate the proposed consumption models two types of experiments have been performed to estimate their accuracy.

On one hand we focused specifically on the accuracy of the energy consumption model of the forward motion using different sensors configurations and implementing or not a localization technique.

On the other hand we address more globally the accuracy of the proposed energy models along a 200 m long patrolling mission, implementing different control schemes and various robot velocities. In the laboratory corridors of

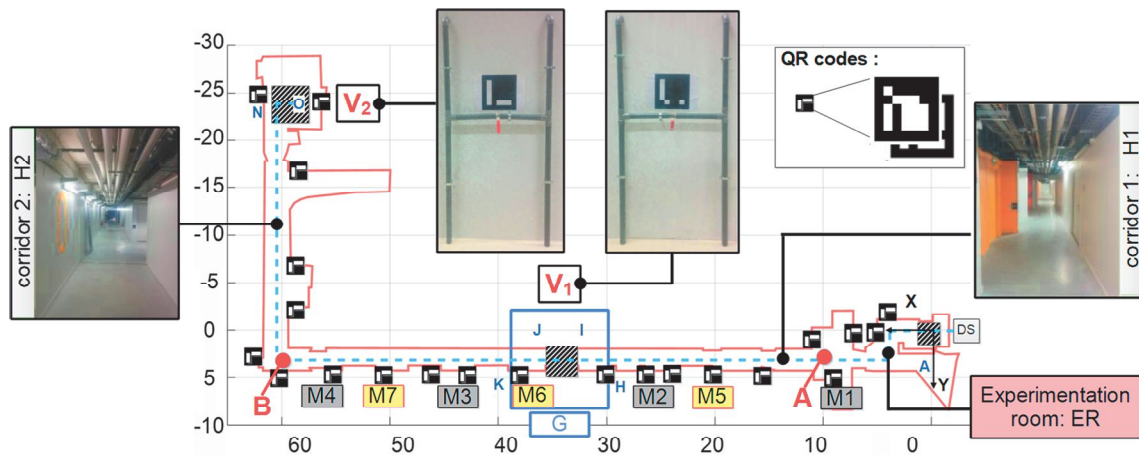


Fig. 3 The experimental context

256 Fig. 3 the mission is to monitor the the state (open or close)
 257 of 2 valves and to go back.

258 The global objectives and consumption identification of
 259 the proposed work being exposed, the next paragraph details
 260 and evaluates the obtained experimental consumption model
 261 of the robot and its on-board laptop.

262 3 Consumption Models and Evaluation

263 This paragraph presents the identification of the instanta-
 264 neous power consumption of the static and dynamic
 265 components. When it is relevant or possible these results are
 266 compared with previous works. Finally the robot and laptop
 267 models are evaluated according to their accuracy.

268 3.1 Robot Battery

269 3.1.1 Static Components

270 Table 2 shows the measured power consumption of the
 271 static components, which remains constant as long as these
 272 sensors are activated.

273 The most energy-consuming sensor is the camera, with
 274 $P_{RKinect} = 2.82$ W. Each of the two laser sensors consumes
 275 $P_{RLaser} = 2.34$ W. Using both lasers requires 4.68 W.
 276 Finally, the measured consumption of the robot controller,
 277 electronic boards and embedded wattmeter when the robot
 278 is not moving $P_{R_Controller1} = 2.67$ W.

Table 2 Power consumption of static components

Static component	Power (W)
Camera	$P_{RKinect} = 2.82$
Robot controller	$P_{R_Controller1} = 2.67$
Hokuyo laser	$P_{RLaser} = 2.34$

279 3.1.2 Dynamic Components

280 Dynamic components are dissipative elements which can be
 281 parametrized at the CS level. We consider in the sequel the
 282 desired forward velocity v that plays an instrumental role
 283 in the motion energy profile, and the recruitment frequency,
 284 denoted f , for the sonar.

285 Firstly we address the motion energy consumption model
 286 that directly impacts the robot battery consumption.

287 DC motor actuators are dynamic components whose
 288 energy consumption depends on the acceleration and
 289 velocity control. The DC motor motion power model for
 290 Pioneer 3DX robots has been widely studied (Sadrpour,
 291 Tokekar, Mei, Kim, etc.). Hereafter we consider the DC
 292 power consumption model of Eq. 5 [1].

$$P_{RMotion}(a, v) = C_1 \cdot a(t)^2 + C_2 \cdot v(t)^2 + C_3 \cdot v(t) + C_4 + C_5 \cdot a(t) + C_6 \cdot a(t) \cdot v(t) \quad (5)$$

293 Often in a robotic mission, the robot path can be divided
 294 into different parts where the velocities of the robot can
 295 be considered constant once the static regime is reached.
 296 Note that the tangential acceleration effects are negligible
 297 by the non-holonomic nature of the unicycle. Hence, robot
 298 acceleration becomes null, and from Eq. 5 only C_2 , C_3
 299 and C_4 parameters remain present. This constant velocity
 300 assumption is usually made at this point in the literature [2,
 301 24, 25] and [21]. The consideration of system dynamics,
 302 as tackled in [14] and [28], results in complex and hard to
 303 manipulate models. Based on this assumption, the motion
 304 power model is simplified in Eq. 6.

$$P_{BRMotion}(v) = C_2 \cdot v^2 + C_3 \cdot v + C_4 \quad (6)$$

305 From experimental measurements (Fig. 4), the analytic
 306 determination of parameters in Eq. 6 leads to:

$$C_2 = 6.25 ; C_3 = 9.79 ; C_4 = 3.66 \quad (7)$$

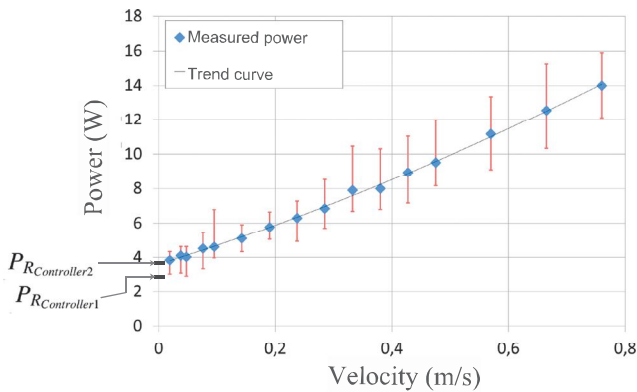


Fig. 4 DC motor motion power versus velocity. Straight forward movement with constant velocities are considered

When the robot does not move, the power is C_4 (3.66 W). This power $P_{R_Controller2}$ corresponds to the steady state consumption required by the different electronic boards, including the embedded wattmeter and the micro-controller within the robot. This constant consumption is removed from experimental data when the consumption model of other hardware components are under study.

Note that normally $P_{R_Controller2}$ would be equal to $P_{R_Controller1}$, but this is not the case. $P_{R_Controller1}$ is in fact obtained using extrapolation. While $P_{R_Controller1}$ is measured by applying motion control using $v = 0$ m/s. Integration of the experimental value $P_{R_Controller1}$ for the determination of Eq. 6 coefficients decreases the quality of the fit. We thus propose the following formulation to model the power consumption:

$$\begin{cases} P_{BR_Motion}(v) = P_{R_Controller1} = 2.67 & \text{if } v = 0 \\ P_{BR_Motion}(v) = 6.25 \cdot v^2 + 9.79 \cdot v + P_{R_Controller2} & \\ = 6.25 \cdot v^2 + 9.79 \cdot v + 3.66 & \text{if } v \neq 0 \end{cases} \quad (8)$$

Hereafter, the quadratic Eq. 6, which must be used when the robot is moving, will only be considered.

Moreover, from Eqs. 2 and 6, considering that $v = d/\Delta T$, where d denotes the travelled distance at constant velocity $v > 0$ during ΔT , the following energy motion modelling equation can apply for the motion energy consumption:

$$E_{R_Motion}(d, v) = C_2 \cdot d \cdot v + C_3 \cdot d + C_4 \cdot \frac{d}{v}. \quad (9)$$

This equation is very interesting and useful since it allows for estimating the motion energy needed to travel over a distance d at velocity v . Figure 5 represents, from Eq. 9, the theoretical motion energy required to travel a distance d at velocity v .

This new curve shows that even if the power consumption is weak for low velocities, the energy consumption needed to travel a given distance increases sharply for low velocities.

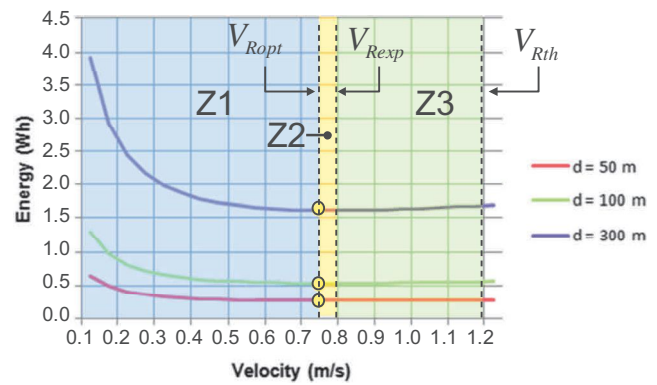


Fig. 5 Motion energy consumption for different distances

These energy curves show a minimum for an optimal velocity V_{Ropt} , which is expressed as:

$$\frac{\partial E_{R_Motion}(d, v)}{\partial v} \Rightarrow V_{Ropt} = \sqrt{\frac{3.66}{6.25}} = 0.76 \text{ m/s} \quad (10)$$

This optimal velocity induces minimum motion energy consumption E_{Ropt} for (V_{Ropt}). Three different areas can be distinguished from these curves.

- Z1 where $v < V_{Ropt}$
- Z2 where $V_{Ropt} < v \leq V_{Exp}$. Note that the maximal velocity cannot be practically reached due to internal default limitation. This induces a significant decrease in the maximal attainable forward velocity of the robot, which is reduced experimentally from $V_{Rth} = 1.2$ m/s to $V_{Exp} = 0.75$ m/s.
- Z3 where $V_{Exp} < v \leq V_{Rth}$. This area can be studied theoretically but cannot be used experimentally for the used robot because of the previous limitation.

A generic formulation of optimal velocity considering the sensor impact is expressed in Eq. 11 using the generic power consumption expressed in Eq. 3, and with the same reasoning as that used previously to establish the optimal velocity.

$$V_{Ropt} = \sqrt{\frac{C_4 + \alpha_2 \cdot P_{RUS}(f) + \beta_1 \cdot P_{R_Kinect} + k_1 \cdot \beta_2 \cdot P_{R_Laser}}{C_2}} \quad (11)$$

On the one hand, many works concerning power consumption modelling are based on electrical and mechanical laws. Kim in [14] conducted a very complete and detailed analysis of the energy consumption of a wheeled mobile robot like the Pioneer 3DX to determine the minimum-energy motion velocity profile, for straight line motion. A close reasoning is proposed in [27] and [28] to build energy optimal velocity profiles for robot DC motors. However, more complex motion paths are considered using a simplification of Eq. 5.

On the other hand, some studies used black box like models directly extracted from experimental measurements.

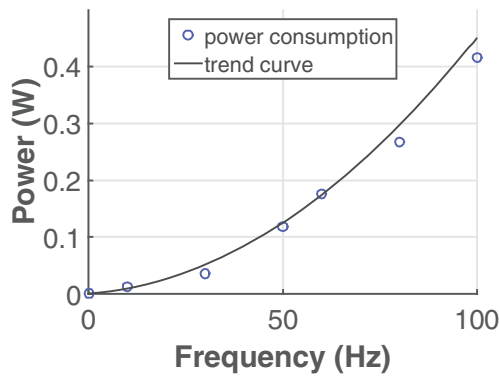


Fig. 6 Power consumption of one sonar cell

370 From the power versus angular velocity curve, the power
 371 behaviour is modelled using a second or sixth-degree polyno-
 372 mial equation whose coefficients are estimated from exper-
 373 imental curves. This approach is used in [31] to estimate the
 374 motion efficiency of different motion plans. Mei et al. in
 375 [31] used the second degree polynomial experimental model
 376 to deploy a set of mobile robots that cover an area under
 377 energy and time constraints. This work was referenced in
 378 Zhang et al. [32, 33] and was also used in Brateman et al. in
 379 [6] to model the power consumption of a Pioneer 3DX robot
 380 to investigate the energy minimization problem.

381 The model proposed in this work clearly belongs to the
 382 second class. However the generic formulation of the robot
 383 battery consumption explicitly integrates the impact of all
 384 the devices used. Moreover the formulation of Eq. 9 and its
 385 use for a given distance of straight movement seems to be
 386 original, putting in light the existence of a robot velocity
 387 minimizing energy consumption. So the proposed model
 388 is a good compromise between hard closed-form equation
 389 which are difficult to manipulate, and more simplistic global
 390 model not very accurate.

391 Secondly, the sonar sensor is another example of dynamic
 392 components because its energy consumption depends on the
 393 frequency rate. The sonar power consumption is experimen-
 394 tally identified and reported in Fig. 6 for different frequencies
 395 f .

396 A polynomial curve trend of Eq. 12 was built from
 397 experimental data.

$$P_{R_{US}}(f) = 4 \cdot 10^{-5} \cdot f^2 + 5.1 \cdot 10^{-4} \cdot f \quad (12)$$

398 Experimentally, the standard working frequency is 25
 399 Hz, which corresponds to $P_{R_{US}}(25) = 0.037W$. The same
 400 study was carried out in [19], but was restricted to a linear
 401 approximation.

402 3.2 Laptop Battery

403 The energy provided by the laptop battery depends on three
 404 main factors: the laptop processor, internal components

such as the hard drive and communication boards, external
 components like the screen and connection devices, such as
 USB.

The processor consumption P_{Proc} has been widely
 studied for CMOS-based chips. CPU power can also be de-
 divided into dynamic and static parts. The Dynamic power
 consumption P_{Dyn} is dissipated when switching activity of
 the processor occurs. This power part can be approached by
 applying a cubic polynomial law of the CPU clock frequency
 when a low voltage level is used for the processor [7]. The
 Static power (or idle power) P_{Stat} corresponds to the power
 consumption when the processor has no tasks to execute. It
 is lower than the dynamic power but not negligible.

This processor power model was used in [32, 33] to
 control the processor frequency for recognition tasks using
 a Pioneer 3DX robot. The same model is used in [6] to
 control the frequency of the processor to reduce energy
 consumption while preventing robot collision.

This initial CPU processor model can be refined
 considering that the static part depends linearly on the
 processor frequency and adding DRAM or cache memory
 access consumption as a constant [15].

The laptop internal components also impact the energy
 consumption. However, these components, such as hard
 disks, network boards (typically 1W [23, 26], etc., consume
 almost constant power [5]. Their standard deviation between
 active and idle activities is generally considered to be small.

External device connection has an important impact on
 energy consumption. Two main sources can be considered.
 The screen display is a major source of consumption
 for a laptop, including backlight [6]. The second is the
 USB connections with external components such as sensors
 (lasers, Kinect), switchboards or robot control processors.
 USB can provide power to low powered peripherals up to
 2.25 W. Depending the type of peripheral, the current can
 reach 0.5 A [16] from the bus for USB 1.x and 2.0 and up
 to 0.9 A for USB 3.x. That corresponds to maximal power
 consumption ranging from 2.5 W to 4.5 W depending on the
 considered USB specification.

From this analysis, it is clear that the laptop battery
 must supply several internal and external components and
 devices. Moreover, depending on the hardware and software
 configuration needed for a CS, the corresponding CPU
 consumption can significantly change.

In the sequel, the laptop battery power consumption
 models are based on detailed analysis of the power
 consumption of the different external hardware devices,
 which are triggered by a given CS. The experimental results
 proposed are based on external experimental measurements
 combined with on-line monitoring of the battery current
 and voltage. Experimental power measures are periodically
 recorded over a time interval. In the following, the processor
 values correspond to the mean of the recorded values.

Table 3 Laptop power consumption of external laptop devices

External device	Power (W)		
Laser	0.400 (each)		
Robot controller	0.075		
Kinect	1.200		
Wattmeter	0.490		
Switch board	no relay activated	1 relay activated	2 relays activated
	0.087	0.405	0.720

458 **3.2.1 Static/External Components**

459 The static consumption of the laptop battery corresponds
 460 to the external links using USB connections. Although the
 461 robot battery externally supplies sensors, USB commu-
 462 nication with the sensors and the switchboards with the
 463 laptop impact the laptop battery consumption. The mea-
 464 sured power consumption, for the different configurations
 465 are summarized in Table 3.

466 **3.2.2 Dynamic/Internal Components**

467 The laptop integrates many internal energy-consuming
 468 devices. This internal consumption depends on many factors
 469 like the currently running processes, hard drive access,
 470 electric fan, wifi board consumption and of course the
 471 laptop processor. Unfortunately it is hard to differentiate the
 472 impacts of each factor. However, as supposed in [20] and
 473 [19], all of these factors can be integrated in a single power
 474 consumption factor P_{LProc} considered as constant for a
 475 given control scheme and external hardware configuration.

476 Table 4, summarizes the experimental data acquired con-
 477 sidering the software and hardware elements involved in
 478 different control schemes. In this table, the control schemes,
 479 their hardware configurations, and their corresponding con-
 480 sumptions are presented horizontally. Vertically, this table
 481 can be divided into different parts : The control scheme,
 482 the involved sensors and actuators, the sensors, actuators,
 483 screen, processor consumption, the robot and laptop bat-
 484 tery consumption and their corresponding percentages. The
 485 locomotion consumption impact was measured by consid-
 486 ering a velocity of 0.1 m/s for RVT and 0.5 m/s for all other
 487 control schemes. All of the different control scheme config-
 488 urations were implemented and tested but, for readability, in
 489 the sequel we present only an analysis focusing mainly on
 490 direct actuation control (FM).

491 The important screen power consumption is measured to
 492 $P_{LScreen}$ is 2.69 W, hence, it must be turned off during a
 493 mission.

3.3 Experimental Evaluation of Energy Consumption Models 494
495

3.4 Control Schemes Consumption : Global Analysis 496

By applying Eq. 3 for different sensor configurations, each
 497 control scheme leads to a very broad power consumption
 498 range, with regard to the robot battery consumption. If we
 499 focus on the Forward Motion control scheme in Table 4,
 500 depending on the chosen configuration, the power consump-
 501 tion can go from 10.12 W to 17.66 W for the 12 possible
 502 choices. The corresponding power consumption difference
 503 between the minimal and maximal values is 74.5%, thus
 504 highlighting the huge energy impact of the selected sensors
 505 on the battery consumption. 506

Overall, in this Table, if all of the proposed CS configura-
 507 tions are considered, the power consumption extracted from
 508 the robot battery can range from 4.7 W (SPF-OA/ODO con-
 509 trol scheme with only the DC motor) up to 17.66 W when
 510 all sensors are mobilised. Note, moreover, that the energetic
 511 impact on the robot battery can be the same for differ-
 512 ent control schemes when the same sensors and actuators
 513 are involved. However, the laptop battery impact will differ
 514 because the algorithms used can differ. 515

Focussing now on the processor power consumption 516
 517 for different hardware configurations. Table 4 shows for
 518 example, for the Forward-Motion CS (FM) that the
 519 consumption ranged from 10.81 W to 13.34 W. Hence,
 520 depending on the sensor configuration (required by the
 521 algorithm use), the same CS power consumption of the
 522 laptop processor can differ up to 23%.

523 Considering all possible control schemes and hardware
 524 combinations, the processor power consumption ranged
 525 from 10.81 W (FM with one laser) up to 14.15 W (CM with
 526 sonars, two lasers and the Kinect).

527 More generally, the robot and laptop power consump-
 528 tions have been combined to estimate the overall power
 529 needs. For the Forward Motion CS, the overall power
 530 needed for the robotic system ranges from 22.23 W to 34.68
 531 W when the screen display is disconnected. The robot and
 532 laptop part are roughly identical. The maximal difference
 533 (9%) is observed for $P_R = 45.49\%$ and $P_L = 54.51\%$. This
 534 result is confirmed for all control schemes and configura-
 535 tions except for the IA and RVT control schemes. For these
 536 tasks, the laptop power consumption represents roughly
 537 70% of the total power needed.

3.4.1 Trajectory Sensibility 538

539 In this part, different motion control schemes are used
 540 to move along the corridor H1 between the A and B
 541 points along 20 or 50 m (Fig. 10). As in many research
 542 studies, straight moving was chosen because most of the
 543

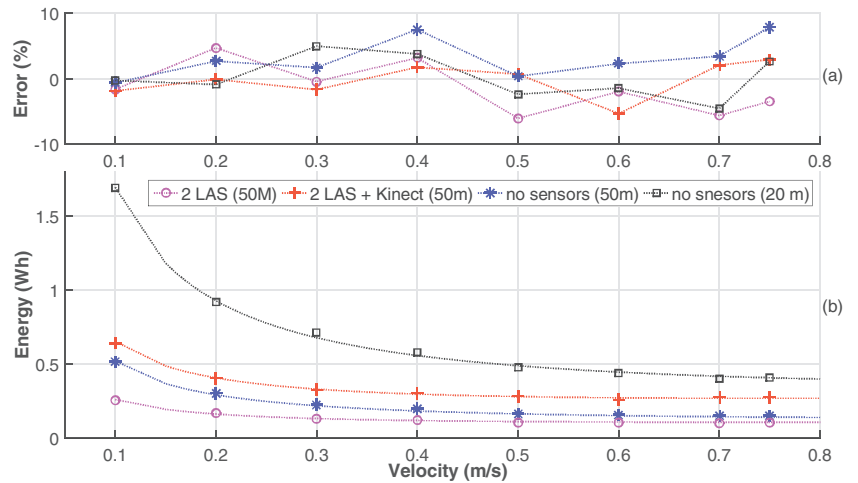
Table 4 Detailed power consumption of the robotic system: Experimental data

	Sensors			Locomotion		Robot Battery	PC Battery												
	US	LAS	KIN	Stop	DC Motor (0.5 m/s)		DC Motor (0.1 m/s)	P_L Kinect	P_L Laser	$P_{watt} + Robot^*$	P_L Switch1	P_L Switch2	P_L screen**	P_L Proc	P_L (W)	%P Screen	$P_{Total} = P_R + P_L$	% P_R	% P_L
<i>RVT</i>	0	0	1	0	0	1	1.20	0.00	0.57	0.09	0.41	2.69	13.38	15.64	14.68	23.16	32.47	67.53	35.06
<i>ODO</i>	0	0	0	0	0	1	0.00	0.00	0.57	0.09	0.09	2.69	11.00	11.74	18.65	16.44	28.60	71.40	42.81
	0	0	0	0	1	0	0.00	0.00	0.57	0.09	0.09	2.69	11.75	12.49	17.72	22.61	44.75	55.25	10.49
<i>QRCN</i>	1	1	1	0	1	0	1.20	0.40	0.57	0.41	0.41	2.69	13.72	16.69	13.88	32.01	47.85	52.15	4.29
	1	2	1	0	1	0	1.20	0.80	0.57	0.72	0.41	2.69	13.27	16.96	13.69	34.62	51.00	49.00	2.01
<i>GBL</i>	0	1	1	0	1	0	1.20	0.40	0.57	0.41	0.41	2.69	13.66	16.63	13.92	31.91	47.88	52.12	4.24
	0	2	1	0	1	0	1.20	0.80	0.57	0.72	0.41	2.69	13.21	16.90	13.73	34.52	51.04	48.96	2.08
<i>FM</i>	1	2	1	0	1	0	1.20	0.80	0.57	0.72	0.41	2.69	13.90	16.37	16.43	31.17	47.48	52.52	5.04
	0	2	1	0	1	0	1.20	0.80	0.57	0.72	0.41	2.69	13.33	17.02	13.65	34.68	50.92	49.08	1.83
	0	2	1	0	1	0	1.20	0.80	0.57	0.72	0.41	2.69	13.27	16.96	13.69	34.58	50.95	49.05	1.90
	1	1	1	0	1	0	1.20	0.40	0.57	0.41	0.41	2.69	13.34	16.31	14.16	31.63	48.43	51.57	3.14
	0	1	1	0	1	0	1.20	0.40	0.57	0.41	0.41	2.69	13.28	16.25	14.20	31.53	48.46	51.54	3.08
	1	2	0	0	1	0	1.20	0.80	0.57	0.72	0.09	2.69	11.54	13.71	16.40	28.55	51.97	48.03	3.94
	0	2	0	0	1	0	1.20	0.80	0.57	0.72	0.09	2.69	11.48	13.65	16.46	28.45	52.02	47.98	4.04
	1	0	1	0	1	0	1.20	0.00	0.57	0.09	0.41	2.69	12.78	15.04	15.17	28.02	46.32	53.68	7.37
	0	0	1	0	1	0	1.20	0.00	0.57	0.09	0.41	2.69	12.72	14.98	15.22	27.92	46.34	53.66	7.31
	1	1	0	0	1	0	1.20	0.40	0.57	0.41	0.09	2.69	10.87	12.33	17.91	24.83	50.33	49.67	0.67
<i>IA</i>	1	0	0	0	1	0	1.20	0.40	0.57	0.41	0.09	2.69	10.81	12.27	17.98	24.73	50.38	49.62	0.76
	1	0	0	0	1	0	1.20	0.00	0.57	0.09	0.09	2.69	11.43	12.17	18.10	22.33	45.49	54.51	9.02
<i>CM</i>	0	0	0	0	1	0	1.20	0.00	0.57	0.09	0.09	2.69	11.37	12.11	18.18	22.23	45.52	54.48	8.96
	0	0	1	1	0	0	1.20	0.00	0.57	0.09	0.41	2.69	11.74	14.00	16.12	19.49	28.17	71.83	43.66
	1	2	1	0	1	0	1.20	0.80	0.57	0.72	0.41	2.69	14.15	17.84	13.10	35.50	49.74	50.26	0.52
	0	2	0	0	1	0	1.20	0.80	0.57	0.72	0.09	2.69	12.30	14.47	15.68	29.27	50.56	49.44	1.12
<i>CM</i>	1	2	0	0	1	0	1.20	0.80	0.57	0.72	0.09	2.69	12.36	14.53	15.62	29.37	50.52	49.48	1.04
	0	2	1	0	1	0	1.20	0.80	0.57	0.72	0.41	2.69	14.09	17.78	13.14	35.40	49.77	50.23	0.46

* $P_{watt} + robot$: Basic consumption when system is stopped

** P_L screen is measured but unused during mission (screen is off)

Fig. 7 a Model error b Experimental and theoretical robot energy consumption



543 time a robot mission involves straight lines with few
544 rotations [14, 31].

545 Firstly we consider a simple Foward Motion without
546 any global localization or obstacle avoidance. Figure 3
547 shows the robot battery energy measured, and the model
548 error for different robot velocities for three external
549 configurations: no sensors used, two lasers or two lasers and
550 the Kinect connected. For energy, the represented points are
551 experimental data. Curves show the theoretical prediction
552 model with and without sensors.

553 The model error is ranged from -6% to +8% while the
554 error mean ranged from -1.41% to +3.14%. The standard
555 deviation was roughly constant at around 3%. As a first
556 evaluation, there was a close fit between the theoretical
557 curves and the experimental measurements (Fig. 7).

558 Concerning the laptop point of view the curves of
559 Figure 8 are obtained. The theoretical curves and experi-
560 mental measurements fit closely too. More precisely, the
561 energy measurements fit the model prediction with an error
562 ranging from -6.6% to 2.6%, and with a negative error mean

of less than 2.8%. The standard deviation was approxi- 563
564 mately 2.5%.

565 These results demonstrate that theoretical laws accurately 566
567 predict the power and energy consumption when forward 568
569 motion is considered and different sensors are connected. 570
571 However the experiment was done in open-loop. That is to 572
573 say that the robot is supposed to follow the imposed path. 574

575 Now, focusing only on robot battery consumption we 576
577 secondly consider that the control periodically adjusts the 578
579 robot velocity and orientation to follow the defined 50 m 580
581 long straight line path with a constant linear forward 582
583 velocity. These experimentations show the impact of the 584
585 closed-loop (control and localization methods) on the actual 586
587 distance travelled and the robot velocity. These conditions 588
589 differ from those used in Kim and Kim [14] and Tokekar 590
591 et al. [28], where the robot was assumed to be permanently 592
593 on the desired path.

594 In a first step the same previous experiment is redone 595
596 with a closed loop control law based only on odometer 597
598 information without any other sensors (dead reckoning). 599
600

Fig. 8 a Model error b Experimental and theoretical laptop energy consumption

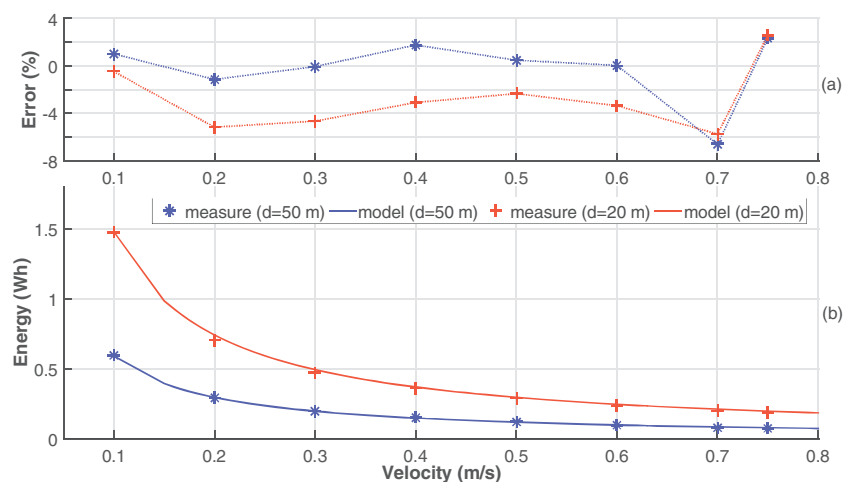


Table 5 Experimental results for different motion controls

	Velocity (m/s)	0.1	0.3	0.5
Energy	Predicted (Wh)	1.30	0.57	0.41
Simple Forward Motion	Experiment (Wh)	1.31	0.54	0.40
	Error (%)	0.53	4.34	0.95
Energy	Predicted (Wh)	1.30	0.57	0.41
Centring Motion	Experiment (Wh)	1.49	0.63	0.48
	Error (%)	12.55	12.99	14.36
Energy Exp. 1	Predicted (Wh)	1.69	0.67	0.48
QR-Code Motion	Experiment (Wh)	1.88	0.78	0.58
	Error (%)	10.10	14.10	17.24
Energy Exp. 2	Predicted (Wh)	1.69	0.67	0.48
QR-Code Motion	Experiment (Wh)	1.86	0.76	0.53
	Error (%)	9.13	11.84	9.43

583 Without global or local localization information, the robot
 584 is unaware of its odometric drift error. In a second step
 585 we implement a Centring Motion control using the lasers
 586 information. The irregularity of the environment generates
 587 a path adaptation inducing a trajectory that differs from
 588 the expected one. Finally the last experiment mixes dead
 589 reckoning with periodic QR-codes relocalization using less
 590 (Exp.1 (M1, M2, M3, M4)) or more markers (Exp.2 (M1 to
 591 M8)) of corridor H1 Fig. 3. Table 5 summarizes the main
 592 results of these different experiments. Values are rounded to
 593 the hundredth.

594 The simple open-loop Forward Motion Control Scheme
 595 shows a limited energy error less than 5% but the robot is
 596 not aware that it doesn't follow the desired path. Logically
 597 for the centring motion a higher error of more than 10%
 598 due to the irregular environment is observed. The QR-
 599 code oriented localization highlights the impact of the
 600 localization frequency on the predicted energy. With QR-
 601 codes roughly located every 6-7 m (Exp. 2), the energy
 602 estimation of around 10% remains acceptable.

The experiments showed of course that the energy prediction errors remains acceptable when the theoretical path corresponds to the one followed by the robot (Simple Path Following). Then, when the robot trajectory deviates from its nominal path (increased distance and time), obviously the prediction error increased (Centring Motion or QR-code Based Localization). In the following, the energy estimation is evaluated for different control schemes during a long-term mission.

3.4.2 Mission Level

In this section, a patrolling mission is considered in the experimental environment of Fig. 3. Starting from the docking station situated in the experimental room (ER), the robot must reach the location of two valves (V1 and V2) across corridors H1 and H2 to determine if the valves are open or closed. Then the robot must go back to the docking station. The path to follow is modelled as a sequence of straight lines. The control laws used ensure smooth

Fig. 9 Mission velocity experimental variations

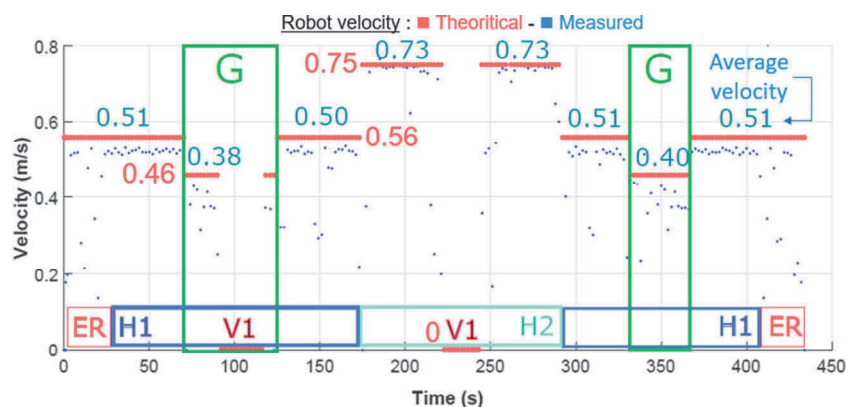
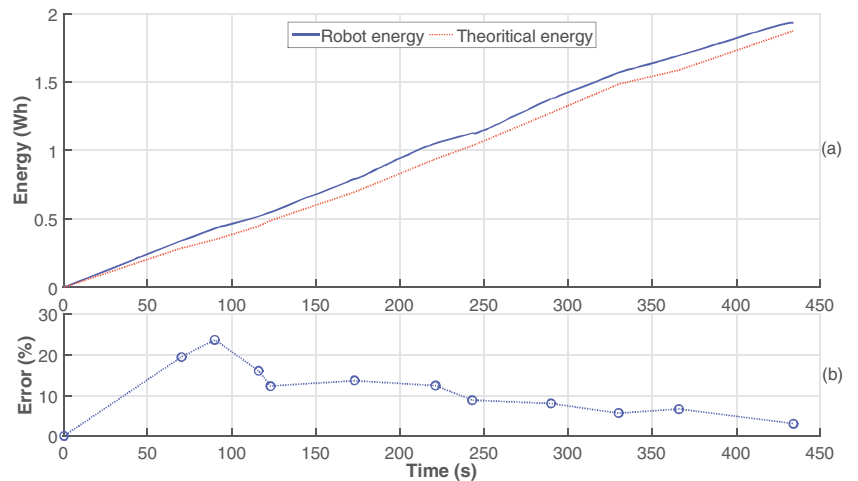


Fig. 10 **a** Mission experimental and theoretical robot energy consumption **b** Robot prediction error for the mission



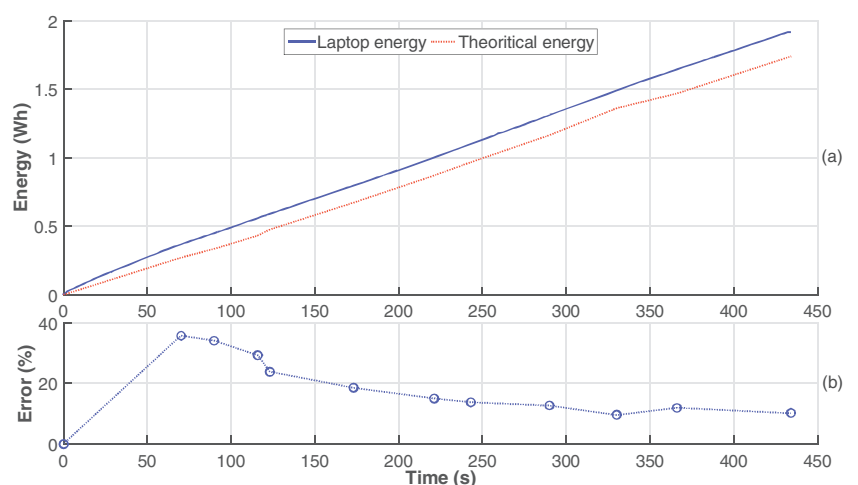
621 path following and different control schemes are used to
 622 realized the mission. The mission is about 180 m long
 623 and takes around 7 minutes. To test the energy estimation
 624 accuracy, different velocities were imposed during the
 625 mission depending on the robot location: mainly 0.46 m/s,
 626 0.56 m/s and 0.75 m/s. Figure 9 presents the theoretical
 627 (red line), measured (blue point) and average robot velocity
 628 during the proposed mission.

629 Differences between the expected and experimental
 630 values were due to the path following control, where the
 631 robot position was periodically corrected to accurately fit
 632 the expected path. In areas where many heading orientation
 633 changes were needed (turns in the experimental room and
 634 valve areas), the gap was around 10%. Due to these bends,
 635 the robot needs to move a quite long distance to stabilise its
 636 trajectory (no heading or velocity change). That explains the
 637 gap of 17.4% near V1 at the beginning of the mission (many
 638 heading orientation changes and short distance), and the
 639 2.7% gap in corridor H2 (few heading orientation changes
 640 and long distance).

641 Figure 10a shows that the experimental robot energy
 642 consumption was slightly higher than expected. However,
 643 the curves are very similar. Moreover, the analysis
 644 illustrated in Fig. 10b demonstrates that the predicted energy
 645 estimation error after an initial peak with an error of 23.7%
 646 decreased to a final 10% error value. The initial peak
 647 was due to the nature of the initial part of the path when
 648 the robot turns a lot to come out the experimental room.
 649 For the rest of the mission, the difference between the
 650 expected path and the real path is small. Moreover, the
 651 energy consumption underestimation (maximal error) at the
 652 beginning of the mission gradually became negligible with
 653 regards to the overall energy consumption as the mission
 654 progressed. Considering the mission overall, the error mean
 655 was 11.5%, with a standard deviation of 6%.

656 The laptop (Fig. 11) and robot energy consumption
 657 curves are similar. The predicted energy was lower than
 658 the experimental energy. The behaviour error showed the
 659 same trend. The observed error was due to the difference
 660 between the real and expected trajectory, which increases

Fig. 11 **a** Mission experimental and theoretical laptop energy consumption **b** Laptop prediction error for the mission



661 the distance and duration necessary to cross the same linear
 662 distance. After an initial peak where the error was 35.9%,
 663 the energy consumption error decreased to 12.1% at the end
 664 of the mission. The mean error was 18.22%, with a standard
 665 deviation of 10.22%, for the overall mission.

666 These analyses demonstrated that the proposed power and
 667 energy consumption models allow a quite good estimation
 668 of the real consumption for missions with many different
 669 control schemes. The underestimation was due to the
 670 difference between the expected and real robot trajectory.
 671 When robot heading orientation changes were not frequent
 672 the consumption estimation was close to the real situation.

673 **4 Conclusion and Future Researches**

674 This paper presents a deep analysis of mobile robot
 675 system power and energy consumption. It focused on a
 676 Pioneer 3DX robot with an embedded laptop. This study
 677 investigated many issues that are seldom addressed in
 678 research studies on this topic.

679 The power and energy consumption of the robot and lap-
 680 top were separately studied distinguishing static and
 681 dynamic components and considering different control
 682 schemes configurations. In the literature the robot battery
 683 is usually only considered, the laptop consumption was
 684 assumed to be constant or was not considered. The impact of
 685 a control scheme configuration on energy consump-
 686 tion is also rarely addressed in the literature. Obviously the
 687 energy consumption clearly closely depends on the mobi-
 688 lized sensors and the chosen algorithms. So, these two sides
 689 of the issue must be considered in a long-term mission.
 690 This study also demonstrates that when the robot is moving
 691 along a straight line of known length with a constant veloc-
 692 ity a simple closed-form relation links these parameters to
 693 the motion energy. Furthermore, to cross a given distance it
 694 exist a velocity minimizing the energy consumption. Finally
 695 experiments confirm the importance of accurate localization
 696 for efficient energy travelling and the good accuracy of the
 697 proposed consumption models along a patrolling mission.
 698 In conclusion, in a known environment, knowing the control
 699 schemes involved during a long-term mission, the models
 700 proposed in this study allow to predict the mission energy
 701 needs with an acceptable gap.

702 There were some obvious shortcomings in this study.
 703 The travelling power consumption model assumes, like many
 704 other studies, that mission can be divided into a set of straight
 705 lines where constant velocities can be applied. This hypothe-
 706 sis is often realistic when known environments are consid-
 707 ered. But the acceleration impact would be integrated into
 708 power consumption models. However the proposed exper-
 709 iment showed that in spite of path following oscillations
 710 and several velocity changes, the power consumption model

preserves acceptable accuracy. For robot field missions, it
 would be harder to meet the objectives due to environ-
 ment variability. But like Sadrpour’s approach [25] the robot
 power motion model could be enhanced by considering
 the impact of the road profile and the road surface condi-
 tions. The correlation between the robot location and power
 consumption should be also studied further in detail. More-
 over, the consumption models are only usable considering
 a known path in a known environment. Finally, from an
 experimental view-point, the identification of the batteries
 power consumption needs an important experimental work.
 All control schemes with all possible sensors and actuators
 configurations must be experimentally studied.

Energy management is clearly a key issue for autonomous
 mobile robots [8]. The findings of this study could be useful
 for addressing many classes of robotic mission issues requiring
 a realistic estimation of robotic system energy consumption.

Energy oriented applications concerns for example
 energy-aware path planning problems as in [29]. However
 more accurate energy estimation models, like the ones
 we have proposed, must be implemented to enhance the
 accuracy of the proposed planning algorithms. So this work
 can help to increase the functioning time of robot systems
 between dockings.

It would be useful to manage energy consumption during
 long-term robotic missions in known environments. Depend-
 ing on the available energy stock, the robotic task control
 and sensor configurations should be adapted throughout the
 mission to ensure that the mission can be completed. Using
 the proposed energy modelling we addressed this issue and
 proposed an approach where the robot can autonomously
 respect many mission performance objectives (Security,
 Energy, mission Duration) using dynamic software and
 hardware resources allocation [11] [12]. More recently in
 [17] the issue considering the links between localization and
 energy was also considered at the mission level.

Finally our on going studies concern underwater robotics
 and exploration missions. Based on this work, we build
 a global and complete energy consumption model for an
 underwater robot, whatever the motion followed and the
 sensors used. The final objectives is to use this energy model
 and our performance management approach to implement
 autonomous karstic exploration. Obviously our predictive
 energy model cannot be used for real exploration of
 underwater caves but it will be essential to decide when to
 stop the exploration part and to manage the way back to the
 meeting point.

Author Contributions Lotfi Jaiem: Conceptualization, Methodology,
 Investigation, Writing - original draft. Didier Crestani: Conceptu-
 alization, Methodology, Data curation, Writing - review and edit-
 ing. Lionel Lapierre: Conceptualization, Methodology, Investigation,
 review and editing. Sebastien Druon: Methodology and Software
 Validation.

764 **Funding** This project was supported by the LabEx NUMEV (ANR-
765 10-LABX-0020) within the I-SITE MUSE (ANR-16-IDEX-0006) and
766 the Region Occitanie (french FEDER funds).

767 **Declarations**

768 **Competing interests** The authors declare that they have no known
769 competing financial interests or personal relationships that could have
770 appeared to influence the work reported in this paper.

771 **References**

772 1. Dc motors, speed controls, servo systems. An engineering
773 handbook Electro-Craft Corporation (1977)

774 2. Asikin, D., Dolan, J.M.: Reliability impact on planetary robotic
775 missions. In: Intelligent Robots and Systems (IROS), 2010
776 IEEE/RSJ International Conference on, pp. 4095–4100. IEEE
777 (2010)

778 3. Aylett, R.: Robots: bringing intelligent machines to life? a quarto
779 book barron's (2002)

780 4. Benini, L., Bogliolo, A., De Micheli, G.: A survey of design tech-
781 niques for system-level dynamic power management. *IEEE Trans.*
782 *VLSI Syst.* **8**(3), 299–316 (2000). [https://doi.org/10.1109/92.845](https://doi.org/10.1109/92.845896)
783 [896](https://doi.org/10.1109/92.845896)

784 5. Bircher, W.L., John, L.K.: Complete system power estimation
785 using processor performance events. *IEEE Trans. Comput.* **61**(4),
786 563–577 (2012)

787 6. Brateman, J., Xian, C., Lu, Y.H.: Energy-efficient scheduling for
788 autonomous mobile robots. IFIP VLSI-SoIC 2006 - IFIP WG 10.5,
789 Int. Conf. VLSI Syst 361–366. [https://doi.org/10.1109/VLSISOC.](https://doi.org/10.1109/VLSISOC.2006.313262)
790 [2006.313262](https://doi.org/10.1109/VLSISOC.2006.313262) (2006)

791 7. Brooks, D.M., Bose, P., Schuster, S.E., Jacobson, H., Kudva,
792 P.N., Buyuktosunoglu, A., Wellman, J., Zyuban, V., Gupta, M.,
793 Cook, P.W.: Power-aware microarchitecture: Design and modeling
794 challenges for next-generation microprocessors. *IEEE Micro*
795 **20**(6), 26–44 (2000)

796 8. Deshmukh, A., Vargas, P.A., Aylett, R., Brown, K.: Towards
797 socially constrained power management for long-term operation
798 of mobile robots (2011)

799 9. Ersal, T., Kim, Y., Broderick, J., Guo, T., Stefanopoulou, A.,
800 Siegel, J., Tilbury, D., Atkins, E., Peng, H., Jin, J., Ulsoy, A.:
801 Keeping ground robots on the move through battery and mission
802 management. *ASME Dyn. Syst. Contr. Magaz.* 1–6. [https://doi.](https://doi.org/10.1115/6.2014-Jun-4)
803 [org/10.1115/6.2014-Jun-4](https://doi.org/10.1115/6.2014-Jun-4) (2014)

804 10. Ishikawa, K., Lu, D.J.: What is total quality control ? : the
805 Japanese way. Prentice-Hall Englewood Cliffs (1985)

806 11. Jaiem, L., Druon, S., Lapierre, L., Crestani, D.: A step toward
807 mobile robots autonomy: Energy estimation models. 177–188
808 (2016)

809 12. Jaiem, L., Lapierre, L., Godary-Dejean, K., Crestani, D.: Toward
810 performance guarantee for autonomous mobile robotic mission:
811 An approach for hardware and software resources management.
812 189–195 (2016)

813 13. Kakogawa, A., Jeon, S., Ma, S.: Stiffness design of a resonance-
814 based planar snake robot with parallel elastic actuators. *IEEE*
815 *Robot. Auto. Lett.* 1–1. [https://doi.org/10.1109/LRA.2018.27972](https://doi.org/10.1109/LRA.2018.2797261)
816 [61](https://doi.org/10.1109/LRA.2018.2797261) (2018)

817 14. Kim, C.H., Kim, B.K.: Minimum-energy motion planning for
818 differential-driven wheeled mobile robots. *Inchopen* 193–226
819 (2008)

820 15. Kim, M., Ju, Y., Chae, J., Park, M.: A simple model for estimating
821 power consumption of a multicore server system. *Int. J. Multimed.*
822 *Ubiquitous Eng.* **9**(2), 153–160 (2014)

16. Kollman, R., Betten, J.: Powering electronics from the usb port. *Analog Applications Journal* 29–35 (2002) 823
824

17. Lambert, P., Lapierre, L., Crestani, D.: An approach for fault tol-
825 erant and performance guarantee autonomous robotic mission. In:
826 13th NASA/ESA conference on adaptive hardware and systems,
827 AHS 2019, pp. 87–94. <https://doi.org/10.1109/AHS.2019.00009>
828 (2019) 829

18. Lapierre, L., Zapata, R.: A guaranteed obstacle avoidance
830 guidance system the safe maneuvering zone. *Auton. Robot.* **32**,
831 177–187 (2012). <https://doi.org/10.1007/s10514-011-9269-5>
832

19. Mei, Y.M.Y., Lu, Y.H.L.Y.H., Hu, Y., Lee, C.: A case study of
833 mobile robot's energy consumption and conservation techniques.
834 ICAR '05. In: Proceedings., 12th International Conference
835 on Advanced Robotics 2005, pp 492–497. [https://doi.org/10.](https://doi.org/10.1109/ICAR.2005.1507454)
836 [1109/ICAR.2005.1507454](https://doi.org/10.1109/ICAR.2005.1507454) (2005) 837

20. Ogawa, K., Kim, H., Mizukawa, M., Ando, Y.: Development
838 of the robot power management system adapting to tasks
839 and environments-The design guideline of the power control
840 system applied to the distributed control robot. In: 2006
841 SICE-ICASE International Joint Conference, pp 2042–2046.
842 <https://doi.org/10.1109/SICE.2006.315489> (2006) 843

21. Parasuraman, R., Pagala, P., Kershaw, K., Ferre, M.: Model based
844 on-line energy prediction system for semi-autonomous mobile
845 robots. In: 5th International conference on intelligent system
846 modelling and simulation, pp 27–29 (2014) 847

22. Passama, R., Andreu, D.: ConTrACT: a software environment for
848 developing control architecture. In: CAR: Control Architectures of
849 Robots. INRIA Grenoble Rhône-Alpes, Grenoble, France. [https://](https://hal.inria.fr/inria-00599683)
850 hal.inria.fr/inria-00599683 (2011) 851

23. Sadrpour, A., Jin, J., Ulsoy, A.G.: Mission energy prediction for
852 unmanned ground vehicles. In: Robotics and Automation (ICRA),
853 2012 IEEE International Conference on, pp. 2229–2234. IEEE
854 (2012) 855

24. Sadrpour, A., Jin, J., Ulsoy, A.G.: Experimental validation of
856 mission energy prediction model for unmanned ground vehicles.
857 In: Proc. 2013 American Contrl Conference, pp 5980–5985 (2013) 858

25. Sadrpour, A., Jin, J.J., Ulsoy, A.G.: Mission energy prediction
859 for unmanned ground vehicles using real-time measurements
860 and prior knowledge. *J. Field Robot.* **30**(3), 399–414 (2013).
861 <https://doi.org/10.1002/rob.21453>
862

26. Sohan, R., Rice, A.C., Moore, A.W., Mansley, K.: Characterizing
863 10 gbps network interface energy consumption. In: IEEE
864 International conference on local computer networks, pp. 268–271
865 (2010) 866

27. Tokekar, P., Karnad, N., Isler, V.: Energy-optimal velocity profiles
867 for car-like robots. In: Robotics and Automation (ICRA), 2011
868 IEEE International Conference on, pp. 1457–1462. IEEE (2011) 869

28. Tokekar, P., Karnad, N., Isler, V.: Energy-optimal trajectory
870 planning for car-like robots. *Auton. Robot.* **37**(3), 279–300 (2014) 871

29. Wei, H., Wang, B., Wang, Y., Shao, Z., Chan, K.C.C.: Staying-
872 alive path planning with energy optimization for mobile robots.
873 *Expert Syst. Appl.* **39**(3), 3559–3571 (2012). [https://doi.org/10.](https://doi.org/10.1016/j.eswa.2011.09.046)
874 [1016/j.eswa.2011.09.046](https://doi.org/10.1016/j.eswa.2011.09.046)
875

30. Xi, W., Remy, C.D.: Optimal gaits and motions for legged
876 robots. In: 2014 IEEE/RSJ International conference on intelligent
877 robots and systems, Chicago, IL, USA, September 14-18, 2014,
878 pp. 3259–3265. IEEE. <https://doi.org/10.1109/IROS.2014.6943015>
879 (2014) 880

31. Mei, Y., Lu, Y.-H., Hu, Y.C., Lee, C.S.G.: In: IEEE International
881 Conference on Robotics and Automation, 2004. Proceedings.
882 ICRA '04. 2004, vol. 5, pp 4344–4349 (2004) 883

32. Zhang, W., Lu, Y.H., Hu, J.: Optimal solutions to a class of power
884 management problems in mobile robots. *Automatica* **45**(4), 989–
885 996 (2009). <https://doi.org/10.1016/j.automatica.2008.11.004>
886

33. Zhang, W.Z.W., Hu, J.H.J.: Low power management for
887 autonomous mobile robots using optimal control. In: 2007 46th
888

Q8

Q9

889 IEEE Conference on Decision and Control, pp 5364–5369.
890 <https://doi.org/10.1109/CDC.2007.4434847> (2007)

Publisher's Note Springer Nature remains neutral with regard to 891
jurisdictional claims in published maps and institutional affiliations. 892

UNCORRECTED PROOF